

Cytokine Profiling of Primary Human Macrophages Exposed to Endotoxin-Free Graphene Oxide: Size-Independent NLRP3 Inflammasome Activation

Sourav P. Mukherjee, Kostas Kostarelos, and Bengt Fadeel*


Graphene-based materials including graphene oxide (GO) are envisioned for a variety of biomedical applications. However, there are conflicting results concerning the biocompatibility of these materials. Here, a question is raised whether GO with small or large lateral dimensions triggers cytotoxicity and/or cytokine responses in primary human monocyte-derived macrophages. GO sheets produced under sterile conditions by a modified Hummers' method are found to be taken up by macrophages without signs of cytotoxicity. Then, multiplex arrays are used for profiling of proinflammatory and anti-inflammatory responses. Notably, GO suppresses the lipopolysaccharide (LPS)-triggered induction of several chemokines and cytokines, including the anti-inflammatory cytokine, interleukin-10 (IL-10). No production of proinflammatory TNF- α is observed. However, GO elicits caspase-dependent IL-1 β expression, a hallmark of inflammasome activation, in LPS-primed macrophages. Furthermore, GO-triggered IL-1 β production requires NADPH oxidase-generated reactive oxygen species and cellular uptake of GO and is accompanied by cathepsin B release and K⁺ efflux. Using THP-1 knockdown cells, a role for the inflammasome sensor, NLRP3, the adaptor protein, ASC, and caspase-1 for GO-induced IL-1 β secretion is demonstrated. Finally, these studies show that inflammasome activation is independent of the lateral dimensions of the GO sheets. These studies provide novel insights regarding the immunomodulatory properties of endotoxin-free GO.

1. Introduction

Graphene-based materials (GBMs) have attracted considerable attention for various applications in science and technology.^[1] Graphene oxide (GO), in particular, is being investigated for

Dr. S. P. Mukherjee, Prof. B. Fadeel
Nanosafety & Nanomedicine Laboratory
Institute of Environmental Medicine
Karolinska Institutet
171 77 Stockholm, Sweden
E-mail: bengt.fadeel@ki.se

Prof. K. Kostarelos
Nanomedicine Laboratory
Faculty of Medical & Human Sciences and National Graphene Institute
University of Manchester
Manchester M13 9PL, UK

 The ORCID identification number(s) for the author(s) of this article can be found under <https://doi.org/10.1002/adhm.201700815>.

DOI: 10.1002/adhm.201700815

various biomedical applications due to its attractive physicochemical properties including a large surface area, ease of surface functionalization, and superior colloidal stability in aqueous media when compared to pristine graphene.^[2,3] However, increasing production and use of GBMs also necessitates careful scrutiny of the impact of such materials on cells and tissues. Understanding the interactions of GBMs with the immune system is of particular importance.^[4] Phagocytic cells of the innate immune system represent the first line of cellular defense against foreign intrusion (microorganisms, particles) and also clear cell debris, thus playing an important role in tissue homeostasis. Macrophages are involved in the initiation, propagation, and resolution of inflammation.^[5] A characteristic feature of macrophages is their ability to respond to environmental stimuli such as cytokines, microbial products, and other modulators; this dynamic process of macrophage functional change is referred to as macrophage polarization.^[6] Hence, inflammatory stimuli such as bacterial lipopolysaccharide (LPS) and interferon- γ (IFN- γ) induce

an inflammatory phenotype that promotes T helper 1 (Th1) effector responses and antimicrobial and tumoricidal properties. Macrophages with this phenotype are considered as “classically activated” macrophages. By contrast, stimulation of macrophages with Th2 cytokines such as interleukin-4 (IL-4) or IL-13 leads to an “alternative” activation state, characterized by decreased ability to produce proinflammatory cytokines and increased phagocytic activity.^[6] In addition, macrophages can be re-educated by further changes in stimuli and this process is called macrophage reprogramming. Mills et al. originally proposed that the M1–M2 dichotomy was an intrinsic property of macrophages associated with a transition from inflammation to healing.^[7] However, recent studies have indicated that the traditional M1–M2 model insufficiently describes macrophage activation; it is also notable that many of the markers used for murine macrophages have not translated to human macrophages.^[8] Indeed, it is erroneous to consider that there are only two types of macrophages and one should instead view M1 (classical) or M2 (alternative) activation states as two extremes on a continuum of activation states.^[9] Diversity and

plasticity of phenotype and function are thus characteristic features of macrophages^[6] and functional skewing occurs under physiological conditions and in pathology (e.g., allergic and chronic inflammation, tissue repair, infection, and cancer).^[9] In addition, recent studies have provided evidence that engineered nanomaterials can perturb macrophage polarization, thus affecting their function.^[10] It is also important to note that the efficiency of uptake of nanoparticles differs between M1 and M2 polarized macrophages. Jones et al.^[11] found that mouse strains that are prone to Th1 immune responses cleared nanoparticles at a slower rate than Th2-prone mice. Interestingly, treating macrophages from Th1-prone mice with cytokines to reprogram them into M2 macrophages increased the particle uptake; conversely, treating macrophages from Th2-prone mice with cytokines to differentiate them into M1 macrophages decreased their particle uptake.^[11] The hematopoietic growth factors, granulocyte macrophage colony-stimulating factor (GM-CSF) and macrophage colony-stimulating factor (M-CSF) are traditionally used to polarize macrophages into “M1” (proinflammatory) or “M2” (anti-inflammatory) phenotypes, respectively.^[7] In the present study, primary human monocyte-derived macrophages were activated using M-CSF. Our previous studies showed that such cells readily engulfed nanosized and micrometer-sized mesoporous silica particles as well as silica-coated iron oxide nanoparticles.^[12,13]

Tschopp and co-workers^[14] published the first study on a molecular platform required for the oligomerization and activation of the proinflammatory protease, caspase-1, which they termed the inflammasome. Since then multiple distinct inflammasomes have been identified, and their assembly is governed by unique pattern-recognition receptors, also called inflammasome sensor molecules, in response to pathogen-associated molecular patterns or endogenous danger signals in the cytosol of the host cell.^[15] Notably, the NLRP3 inflammasome also responds to particulate and crystalline matter including silica and aluminum crystals, and asbestos,^[16–19] and a variety of engineered nanomaterials including carbon nanotubes (CNTs).^[20] The oligomerization of NLRP3 usually requires two signals: a priming signal that results in the transcription of inflammasome components, as well as pro-caspase-1, pro-IL-1 β , and pro-IL-18; and a second signal that mediates activation of the inflammasome, such as membrane disruption, reactive oxygen species (ROS) generation, etc.^[15] Inflammasome activation leads to the activation of pro-caspase-1 to caspase-1, which then converts pro-IL-1 β to IL-1 β . Wang et al.^[21] demonstrated IL-1 β secretion in THP-1 cells exposed to single-walled CNTs, graphene, and GO, but a specific role for the NLRP3 inflammasome was not proven.

Previous studies have provided contrasting results on the biocompatibility of GO toward immune-competent cells. Sasidharan et al.^[22] showed that GO was noncytotoxic for murine macrophage-like RAW264.7 cells at doses up to 75 $\mu\text{g mL}^{-1}$, while Ma et al.^[23] reported that GO elicited size-dependent cytotoxicity toward murine macrophage-like J774A.1 cells with a progressive loss of cell viability starting at 20 $\mu\text{g mL}^{-1}$. Orecchioni et al.^[24] also noted a reduction in cell viability in human peripheral blood mononuclear cells exposed to high doses (75 $\mu\text{g mL}^{-1}$) of GO of different lateral dimensions. Using human monocyte-like THP-1 cells, Wang et al.^[21] found that GO was noncytotoxic at doses up to 100 $\mu\text{g mL}^{-1}$, as evidenced

by using the lactate dehydrogenase (LDH) release assay, while Cho et al.^[25] reported a size- and dose-dependent cytotoxicity of GO using the same assay, with a significant loss of cell viability starting at 20 $\mu\text{g mL}^{-1}$, both for single-layer and multi-layer GO. Here we studied whether single-layer GO with small (GO-S) or large (GO-L) lateral dimensions triggered cytotoxicity and/or cytokine responses in primary human monocyte-derived macrophages. GO samples were first tested for endotoxin content. Macrophages were incubated in medium alone or subjected to LPS priming prior to incubation with GO. We observed that GO alone did not elicit proinflammatory effects in macrophages, while pronounced, size-independent IL-1 β secretion as well as skewing of cytokine responses were noted in macrophages upon LPS priming. These data show that GO can induce potent immunomodulatory effects in primary human macrophages.

2. Results

2.1. GO is Noncytotoxic for Primary Human Macrophages

To assess whether the lateral size of GO plays a role for the interaction with macrophages, GO-S and large GO-L produced by a modified Hummers' method were studied. The synthesis and characterization of the samples investigated has been reported in detail.^[26] Thus, small (50–300 nm) and large (10–40 μm) GO samples, one or two layers thick (1–2 nm) with a strongly negative surface charge (ζ -potential, -55 mV) were produced. When these GO samples were dispersed in cell culture medium, an agglomeration was noted, and the ζ -potential appeared less negative, possibly due to the presence of serum proteins, though both GO-S and GO-L remained negatively charged (Figure S1, Supporting Information). Previous studies on single-layer GO prepared by using similar protocols were conducted using a lung cell line (A549)^[27] or T cell (Jurkat) and monocyte-derived (THP-1) cell lines.^[24] In the present study, primary human monocytes differentiated into macrophages using recombinant M-CSF were employed. We and others have shown that such macrophages are more proficient in uptake of silica and gold nanoparticles.^[28,29] We determined the cell viability of human monocyte-derived macrophages (HMDM) exposed to GO-S and GO-L for 24 h by using the Alamar Blue assay which is based on resazurin, a nonfluorescent indicator dye which is converted to red-fluorescent resorufin through reduction reactions of metabolically active cells. These experiments, performed with cells from several different donors, indicated no cell viability loss up to 75 $\mu\text{g mL}^{-1}$ (Figure S2, Supporting Information). Based on these results, a noncytotoxic dose (50 $\mu\text{g mL}^{-1}$) of GO-S and GO-L was selected for subsequent studies. Endotoxin contamination of the test material may produce artefacts, which could skew the results, especially when studying effects on immune-competent cells.^[30] Therefore, we checked the GO samples for endotoxin content using the tumor necrosis factor- α (TNF- α) expression test (TET).^[31] The assay showed a negligible amount of TNF- α expression in HMDM exposed to GO-S and GO-L, and the expression of TNF- α was not affected by polymyxin-b sulfate, indicating that these samples were endotoxin-free (Figure S4A, Supporting Information). LPS (0.1 $\mu\text{g mL}^{-1}$) was used as a positive control and TNF- α secretion was completely blocked by polymyxin-b sulfate (10 $\times 10^{-6}$ M).

2.2. GO is Readily Internalized by Primary Macrophages

Previous studies using murine (J774.A1) or human (THP-1) macrophage-like cell lines have suggested that small GO sheets are readily taken up by cells while large GO showed a stronger adsorption onto the plasma membrane with less phagocytosis.^[23] To study cellular interactions and/or uptake, we performed transmission electron microscopy (TEM) of HMDM exposed to $50 \mu\text{g mL}^{-1}$ of GO-S or GO-L. GO-S (Figure 1B) and GO-L (Figure 1C) were both internalized without any ultrastructural signs of cell death. Unexposed cells are shown in Figure 1A. At high magnification, both

GO-S (Figure 1E) and GO-L (Figure 1F) are seen as neatly folded “packages” inside the cell. In Figure 1E, the entry of sheets of GO-S into the cell is also visualized. Similarly, in Figure 1G, the entry of a “swarm” of micrometer-sized GO-L into cells is visualized. Unexposed cells are shown at higher magnification in Figure 1D, for comparison. Finally, at higher magnification, representative examples of internalized GO-S (Figure 1H) and GO-L (Figure 1I), respectively, in the cytoplasm are seen; no evidence of any gross disturbance of cell morphology was noted. Moreover, upon examination of these and numerous other images, no evidence of adsorption of GO onto the plasma membrane was observed. These data

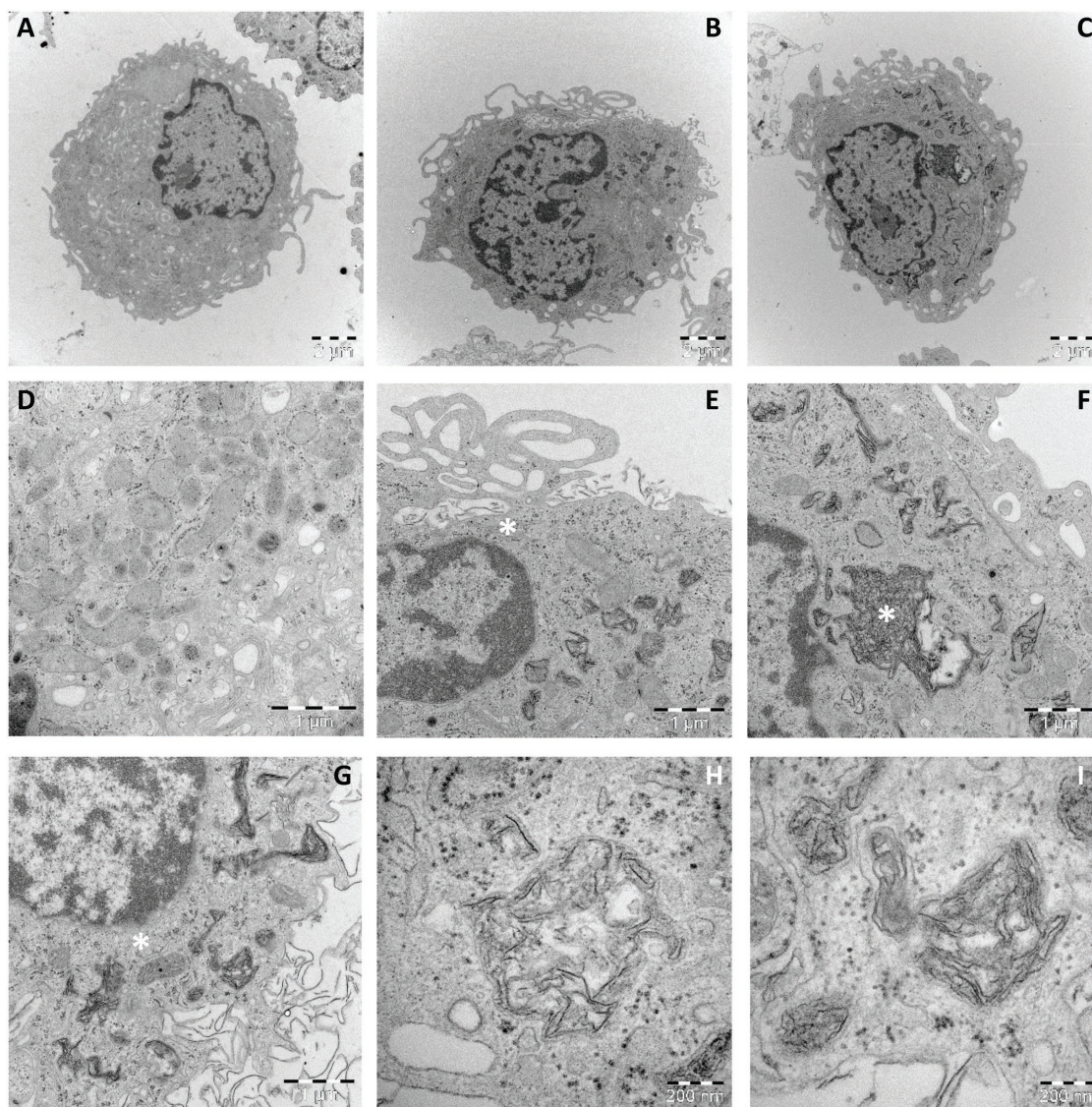


Figure 1. Primary human macrophages readily ingest GO. Human monocyte-derived macrophages activated with M-CSF were incubated with or without GO-S and GO-L ($50 \mu\text{g mL}^{-1}$) for 3 h. TEM micrographs (scale bar: $2 \mu\text{m}$) show a) control cells, b) cells exposed to GO-S, c) cells exposed to GO-L. Internalized GO can be seen in panel (b) and panel (c). Higher magnification micrographs (scale bar: $1 \mu\text{m}$) show d) control cells, e) cells exposed to GO-S, f,g) cells exposed to GO-L. The asterisk in panel (e) indicates GO sheets that are undergoing internalization. The asterisk in panel (g) shows a large aggregation of GO inside the cell while the image in panel (g) shows the presence of GO sheets at the plasma membrane of the cell as well as GO internalized within the cell. The asterisk marks a mitochondrion, for comparison. Finally, at higher magnification (scale bar: 200 nm), the micrographs in panels h) and i) show the structure of internalized GO-S and GO-L, respectively. There were no ultrastructural signs of cell death in GO-exposed cells.

clearly demonstrated that primary macrophages are capable of ingesting GO and that this occurred independent of the lateral dimensions of GO.

2.3. GO Exposure Skews Cytokine Responses in Macrophages

Next we performed multiplex analyses to investigate cytokine and chemokine responses in HMDM exposed to GO-S or GO-L. For these studies, HMDM were primed or not with LPS

($0.1 \mu\text{g mL}^{-1}$) in order to explore the effects of GO on resting/quiescent and activated macrophages. HMDM with or without LPS priming were thus exposed for 24 h to GO-S or GO-L at $50 \mu\text{g mL}^{-1}$ and samples were analyzed using a 27-plex cytokine panel including typical Th1 and Th2 cytokines, chemokines, and growth factors.^[28] LPS ($0.1 \mu\text{g mL}^{-1}$) was included as a positive control. Focusing first on the effects of GO alone, these experiments showed that GO did not trigger the production of the classical proinflammatory Th1 cytokines, TNF- α , IL-6, or IL-1 β in macrophages (Figures 2 and 3; Figure S3, Supporting

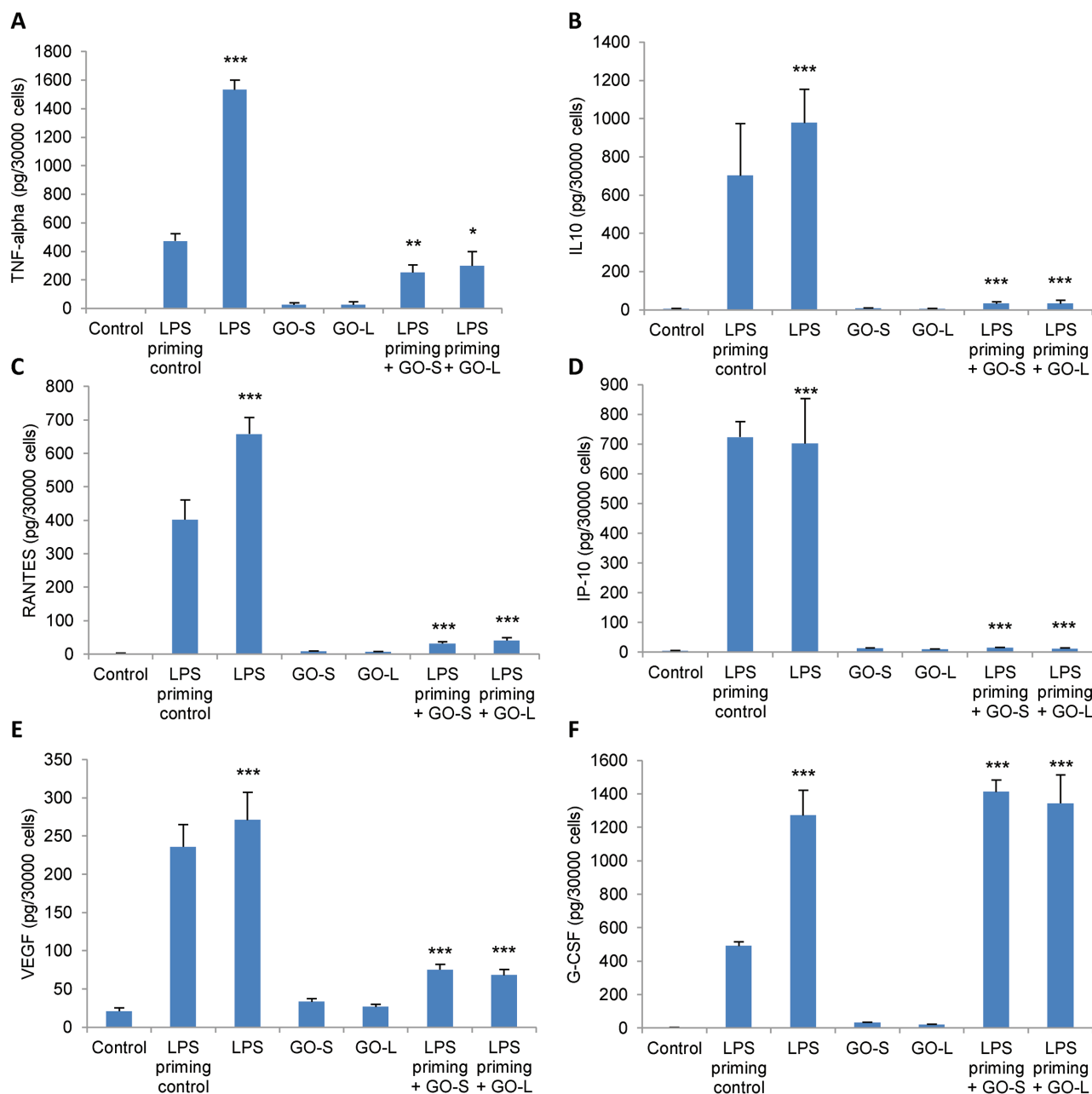


Figure 2. GO is not proinflammatory per se, but skews cytokine secretion in LPS-primed macrophages. Human monocyte-derived macrophages activated with M-CSF and primed or not with LPS (100 ng mL^{-1}) for 2 h were incubated with or without GO-S and GO-L ($50 \mu\text{g mL}^{-1}$) for 24 h, at which time the production of cytokines, chemokines, and growth factors was determined by using the Bio-Plex Human 27-Plex Cytokine Array (for additional results, refer to Figure 3 and Figure S3, Supporting Information). Data shown are mean values \pm S.D. using cells isolated from three individual human donors. *** $P < 0.0001$; ** $P < 0.01$, * $P < 0.05$.

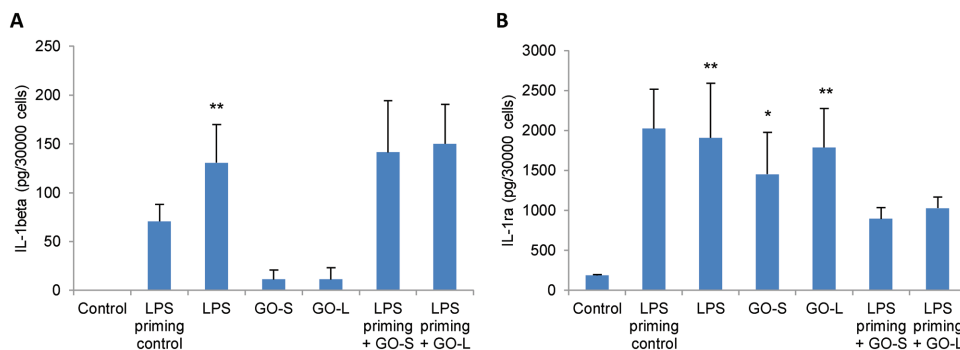


Figure 3. GO (small and large) modulates IL-1 β and IL-1RA secretion in macrophages. Human monocyte-derived macrophages activated with M-CSF and primed or not with LPS (100 ng mL⁻¹) for 2 h were incubated with or without GO-S and GO-L (50 μ g mL⁻¹) for 24 h, at which time the production of IL-1 β and IL-1RA was determined by multiplex array. Data shown are mean values \pm S.D. using cells from three individual human donors. ** $P < 0.01$, * $P < 0.05$.

Information). However, GO induced the production of proinflammatory IL-8/CXCL8, an important chemotactic factor for neutrophils, but not to the same degree as LPS (Figure S3, Supporting Information). Furthermore, GO elicited a small, yet statistically significant increase in the production of IL-17, a proinflammatory cytokine with important roles in antibacterial and antifungal immunity, and IFN- γ , an important Th1 cytokine which plays a key role in the defense against intracellular parasites (Figure S3, Supporting Information).

With regard to typical Th2 cytokines, such as IL-4, IL-5, and IL-13, no effects were noted in cells exposed to GO alone (i.e., in the absence of LPS priming) (Figure S3, Supporting Information). Additionally, GO alone did not stimulate the production of IL-10, an important Th2 cytokine with multiple, pleiotropic immunomodulatory effects^[32] (Figure 2). However, GO triggered a strong upregulation of IL-1 receptor antagonist (IL-1RA), comparable to the effect of LPS (Figure 3). With respect to macrophage production of chemokines, the response to GO was variable. Hence, no effects were noted for RANTES (also known as CCL5) or IP-10/CXCL10 (Figure 2) nor on MIP-1 α (also known as CCL3) (Figure S3, Supporting Information) while production of MIP-1 β (also known as CCL4) and MCP-1 (also known as CCL2) was triggered by GO (Figure S3, Supporting Information). GO showed no or only minor effects on macrophage production of the growth factors, G-CSF, GM-CSF, vascular endothelial growth factor (VEGF), fibroblast growth factor (FGF), or platelet derived growth factor (PDGF) in M2 polarized macrophages with no LPS priming (Figure 2; Figure S3, Supporting Information).

By contrast, when looking at the effects of GO in LPS-activated macrophages, we noted a strong effect of GO on several different cytokines, chemokines, and growth factors. Hence, GO completely suppressed the production/secretion of IL-10 in LPS-primed cells (Figure 2). GO also completely blocked the production of the two chemokines, RANTES (CCL5) and IP-10/CXCL10 in LPS-primed macrophages (Figure 2). Furthermore, the production of VEGF was significantly reduced while the production of G-CSF, a growth factor with multiple immunomodulatory effects, was significantly increased in LPS-primed cells exposed to GO (Figure 2). GO also induced a small, yet statistically significant reduction in TNF- α in LPS-activated cells. The effects of GO in LPS-activated cells could not be explained by a general inhibition of LPS signaling since

several other cytokines, chemokines, and growth factors were unaffected (Figure S3, Supporting Information). Finally, we noted that cells exposed to GO alone expressed low levels of IL-1 β and high levels of IL-1RA, while the opposite trend was observed in LPS-activated cells, i.e., IL-1 β was increased and IL-1RA levels were reduced (Figure 3). Overall, based on this comprehensive analysis, no evidence for lateral dimension-dependent effects of GO was noted. Thus, the identical effects (or lack of effects) were seen for GO-S and GO-L in this model.

2.4. GO and LPS Effects on Cytokine Production are Distinct

To further analyze the macrophage responses to GO, we performed hierarchical clustering analysis to draw association dendrograms between cytokine responses evidenced for GO-S, GO-L, and LPS versus control in HMDM primed or not with LPS (Figure 4). Interestingly, distinct differences were observed with respect to the cytokine-chemokine expression patterns elicited by LPS versus GO in nonprimed cells. Moreover, in LPS-primed cells, LPS and GO also produced distinct expression patterns. Thus, this analysis of the cytokine profiling results has clearly demonstrated that the effects of endotoxin-free GO are different from the effects of LPS. The clustering analysis also suggested that the cytokines could be broadly separated into two clusters: those that were affected by LPS and those affected by GO in cells that were first primed with LPS (Figure 4).

2.5. GO-Induced IL-1 β Secretion is Caspase-Dependent

The cytokine profiling experiments showed that GO triggered IL-1 β production in LPS-primed cells. To further investigate IL-1 β signaling in this model, we studied IL-1 β production in HMDM with or without LPS priming by using a specific enzyme-linked immunosorbent assay (ELISA). Inflammation-dependent IL-1 β production requires caspase-1 activation while caspase-8 was reported to play an auxiliary role.^[33] Therefore, HMDM were preincubated with inhibitors of caspase-1 and -8, or a pan-caspase inhibitor. As shown in Figure 5A, preincubation of HMDM with the pan-caspase inhibitor, zVAD-FMK reduced GO-triggered IL-1 β production to

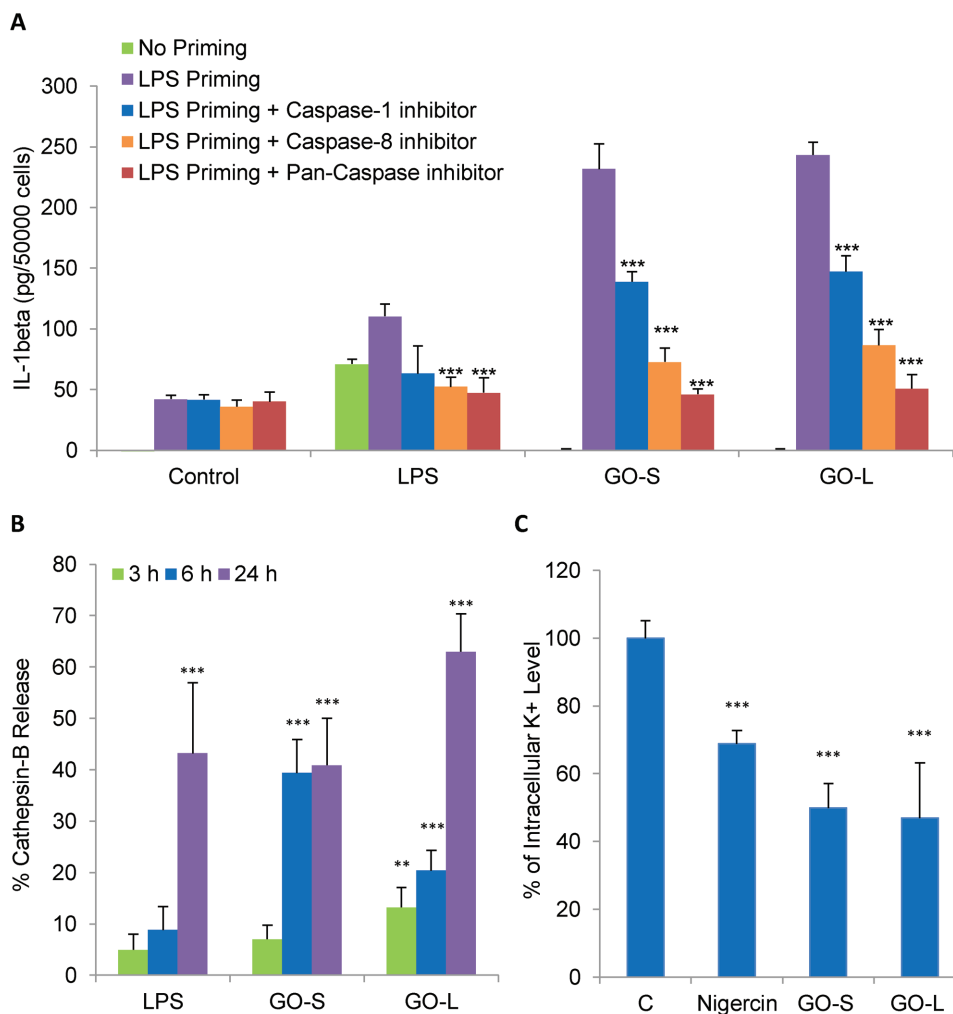


Figure 5. GO triggers caspase-dependent IL-1 β secretion in LPS-primed macrophages. a) Human monocyte-derived macrophages, primed or not with LPS (100 ng mL⁻¹) for 2 h prior to exposure, were incubated with or without GO-S and GO-L (50 μ g mL⁻¹) for 24 h and IL-1 β secretion was determined by using a specific ELISA. Cells were preincubated with a caspase-1 inhibitor (Z-YVAD-FMK, 10 \times 10⁻⁶ M), caspase-8 inhibitor (Z-IETD-FMK, 20 \times 10⁻⁶ M), or the pan-caspase inhibitor, zVAD-FMK (20 \times 10⁻⁶ M) as indicated. b) Lysosomal release of cathepsin B was determined in cells incubated with LPS (0.1 μ g mL⁻¹) versus GO-S and GO-L (50 μ g mL⁻¹) for the indicated time-points by using the Magic Red assay. c) Intracellular K⁺ ion (K⁺) concentrations were determined by using the K⁺ sensitive dye, PBFI-AM, in LPS-primed macrophages following exposure to GO-S and GO-L (50 μ g mL⁻¹) for 24 h. Nigericin (15 \times 10⁻⁶ M) was used as a positive control. Data shown are mean values \pm S.D. using cells from three individual human donors. *** P < 0.0001; ** P < 0.01, * P < 0.05.

macrophage internalization of GO followed by NADPH oxidase activation and ROS production.

2.8. GO Triggers Canonical Inflammasome Activation

The nucleotide-binding and oligomerization domain (NOD)-like receptor, NLRP3, its adaptor apoptosis-associated speck-like protein containing a CARD (ASC), and the effector enzyme, caspase-1, are critical components of the NLRP3 inflammasome complex.^[15] Therefore, we next investigated whether GO-S and GO-L specifically required the NLRP3–ASC–caspase-1 platform for IL-1 β production. To this end, we compared the effects of GO in THP-1 cells with stable knockdown of NLRP3 (def-NLRP3), ASC (def-ASC), or caspase-1 (def-CASP1) versus THP-1 wild-type cells (Null-1). As shown before in primary human macrophages, GO-S

and GO-L did not trigger any IL-1 β production in nonprimed cells (Figure 7A). By contrast, in LPS-primed THP-1 cells, both GO-S and GO-L triggered IL-1 β . Moreover, the level of IL-1 β secretion in Null-1 cells was identical for both small and large GO. Notably, IL-1 β secretion was completely abolished in cells deficient for NLRP3, ASC, and caspase-1 (Figure 7B). The LPS-triggered release of IL-1 β was also blocked in these cells.

3. Discussion

Macrophages play crucial roles in host defense, inflammation, and tissue homeostasis. Macrophages can undergo functional changes in response to their microenvironment and this dynamic process is defined as macrophage polarization.^[6] In the present study, we have demonstrated that endotoxin-free

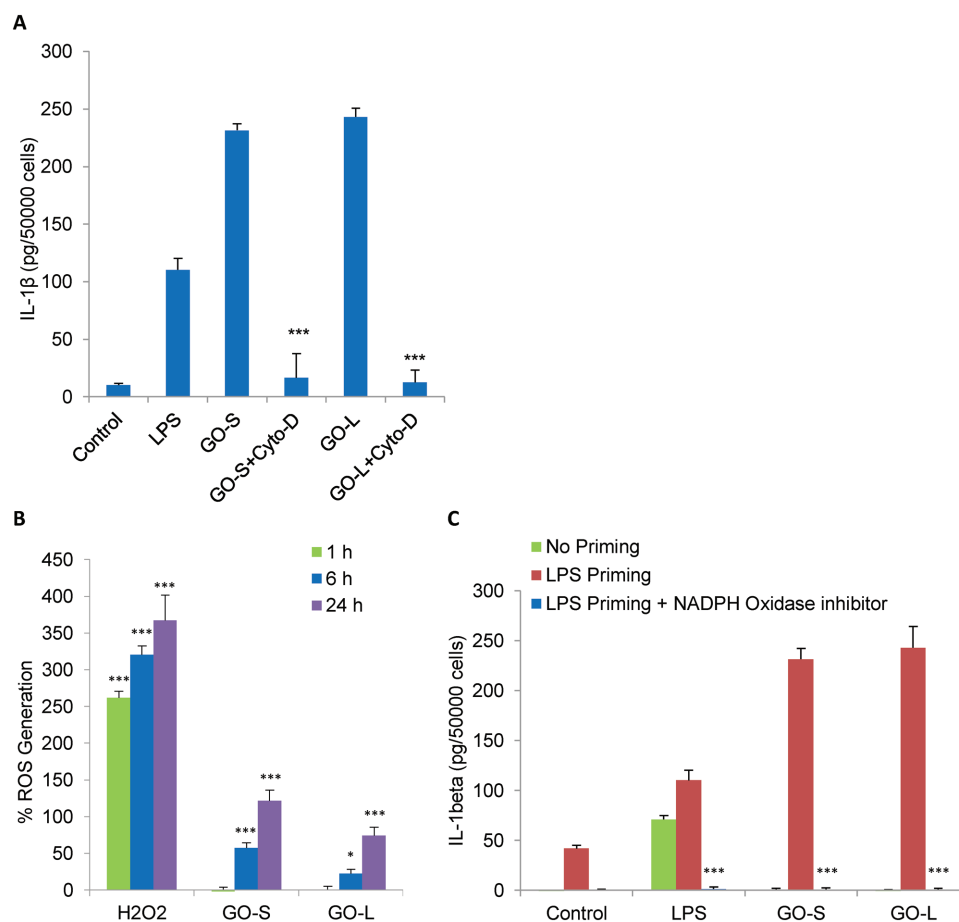


Figure 6. GO-triggered IL-1 β secretion is ROS-dependent and requires phagocytosis of GO. a) LPS-primed human monocyte-derived macrophages were incubated with LPS (0.1 $\mu\text{g mL}^{-1}$) or GO-S and GO-L (50 $\mu\text{g mL}^{-1}$) for 24 h and IL-1 β secretion was determined by using a specific ELISA. Preincubation of the cells with cytochalasin D (10 $\times 10^{-6}$ M) significantly suppressed IL-1 β secretion, as determined by using a specific ELISA. b) ROS production determined by using the H2DCFDA assay showed a time-dependent increase in ROS generation in LPS-primed macrophages exposed to GO-S and GO-L (50 $\mu\text{g mL}^{-1}$). Hydrogen peroxide (100 $\times 10^{-6}$ M) was included as a positive control. c) Macrophages (naïve or primed with 0.1 $\mu\text{g mL}^{-1}$ LPS for 2 h prior to exposure) were incubated with LPS (0.1 $\mu\text{g mL}^{-1}$) versus GO-S or GO-L (50 $\mu\text{g mL}^{-1}$) and the production of IL-1 β was determined by using a specific ELISA. Preincubation with the NADPH oxidase inhibitor, DPI (10 $\times 10^{-6}$ M) completely blocked LPS- and GO-triggered IL-1 β production. Data shown are mean values \pm S.D. using cells derived from three individual human donors. *** $P < 0.0001$; ** $P < 0.01$, * $P < 0.05$.

GO of differing lateral dimensions is noncytotoxic toward primary human macrophages; we also documented significant immunomodulatory effects of GO and could show that GO triggers inflammasome activation in LPS-primed macrophages. Several previous studies have shown that nanoparticles can perturb the polarization of macrophages, thereby affecting their function. Lucarelli et al.^[39] showed that the basal and LPS-induced production of cytokines is subject to modulation in macrophage-differentiated U937 cells exposed to nanoparticles. For instance, SiO₂ nanoparticles were found to selectively induce the production of IL-1 β and TNF- α in naïve cells and amplified the inflammatory phenotype of LPS-polarized cells.^[39] Using primary murine bone marrow-derived macrophages, Kodali et al.^[40] found that superparamagnetic iron oxide nanoparticles caused a transcriptional reprogramming of macrophages leading to a phenotype characterized by an impaired ability to transition from M1 to M2, with suppressed IL-10 induction, enhanced TNF- α production, and diminished phagocytic activity toward bacteria. Furthermore, using primary

human monocyte-derived macrophages, Fuchs et al.^[41] recently reported that both cationic and anionic surface functionalized polystyrene nanoparticles skewed the M2 macrophage polarization (suppression of IL-10) without affecting M1 markers (TNF- α , IL-1 β). It has also been suggested that GO could induce M1 macrophage polarization, using human THP-1 cells and murine J774.A1 cells as a model, with size-dependent production of the proinflammatory cytokines, TNF- α and IL-6, and dose-dependent induction of cell death.^[23] Furthermore, TLR signaling was invoked to account for the effects of GO.^[37] However, in the present study, we did not observe any induction of proinflammatory cytokines (TNF- α , IL-1 β , IL-6) in primary human monocyte-derived macrophages exposed to GO, nor did we observe any cell death. Using specific reporter cell lines, we could not find any evidence for TLR activation by small or large GO sheets. On the other hand, GO-S and GO-L were found to skew cytokine responses in LPS-primed macrophages in as much as GO suppressed the LPS-triggered secretion of the important anti-inflammatory cytokine, IL-10, as well as the

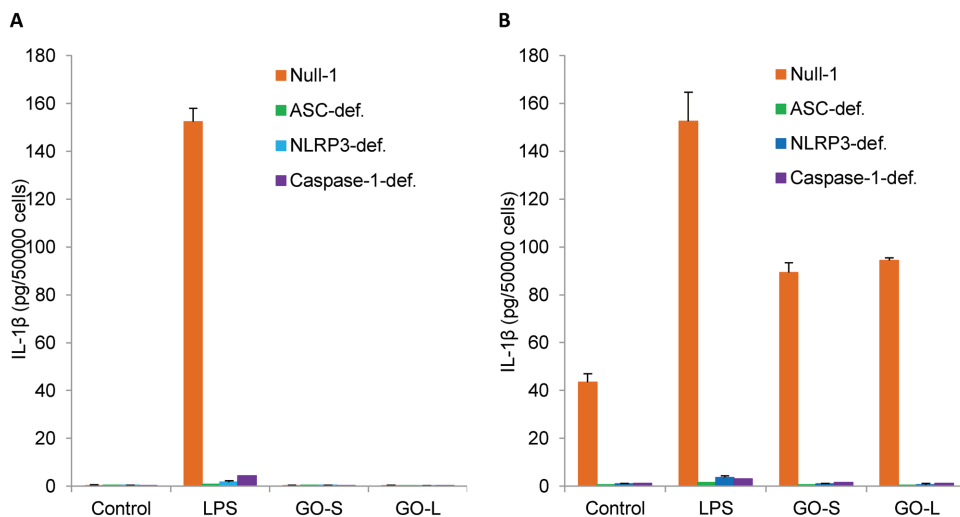


Figure 7. GO (small and large) triggers canonical NLRP3 inflammasome activation. IL-1 β expression was measured in a) nonprimed and b) LPS-primed (2 h) THP-1 wild-type (Null-1) or knockdown cells (ASC-deficient, NLRP3-deficient, or caspase-1-deficient), after exposure to GO-S and GO-L (50 $\mu\text{g mL}^{-1}$) for 24 h. GO-S and GO-L induced IL-1 β secretion in this model, but only after LPS priming, and IL-1 β production was dependent on ACS, NLRP3, and caspase-1.

production of several other cytokines, chemokines, and growth factors. We also noted that GO triggered the production of high levels of IL-1RA and low levels of IL-1 β in naïve macrophages, while in LPS-primed macrophages, IL-1 β was increased and IL-1RA levels were reduced in the presence of GO. Moreover, hierarchical clustering analysis of the cytokine profiling results clearly demonstrated that the effects of GO were distinct from the effects of LPS in this cell model. Human primary monocytes were suggested as reliable models for investigating the effects of engineered nanomaterials on human innate immune responses.^[42] In addition, it is of utmost importance to control for potential endotoxin contamination in studies of GBMs,^[31] in order to guide the data interpretation, in particular when assessing cytokine responses and/or signaling via pattern recognition receptors such as TLRs.

Indeed, while previous studies have suggested that the lateral dimensions play an important role for the cellular responses to GO,^[23,24] it is important to consider not only the physicochemical properties of the test material but also the choice of cell model. Numerous studies on GO were conducted using commonly used cell lines of human or murine origin, such as the lung cell lines, A549^[27,43] and BEAS-2B,^[21,43] or the monocyte-macrophage-like cell lines, THP-1,^[21,24,25] J774A.1,^[23,37] and RAW264.7.^[22,37] and the results may not be directly applicable to primary cells although such studies are useful for screening purposes and/or for mechanistic studies. In the present study, we found that both GO-S and GO-L were noncytotoxic for primary human monocyte-derived macrophages at concentrations up to 75 $\mu\text{g mL}^{-1}$. In fact, we found that cellular metabolism of the indicator dye, resazurin, was enhanced in cells exposed to GO when compared to untreated controls. It is pertinent to note that previous studies in which cells were grown on GO-coated surfaces have revealed that GO enhances the attachment and proliferation of various cancer cell lines.^[44,45] In a previous study using primary human monocyte-derived macrophages and primary murine peritoneal macrophages, GO

sheets were shown to have a tendency to interact with the plasma membrane, especially of the murine macrophages, and seemed to orient themselves parallel to the cell surface (so-called “masking” effect).^[46] The authors hypothesized that this contact between GO sheets and the cell membrane could promote their internalization, or isolate or encase the cells, thereby accounting for the subsequent cellular responses including loss of cell viability and cytokine secretion.^[46] Interestingly, the proinflammatory cytokines, TNF- α and IL-1 β , were secreted by murine macrophages, but not by human macrophages, in response to GO.^[46] Using macrophage-differentiated THP-1 cells as a model, Cho et al.^[25] observed dose-dependent cytotoxicity in response to single-layer GO and could show that cell death was dependent on phagocytosis. In the present study, GO-S and GO-L were both internalized by primary human macrophages without signs of cell death and we did not observe any “masking” of the cell membrane. It is important to note that macrophages are professional phagocytes specialized in engulfing dying cells and cell debris.^[47] Moreover, we have previously shown that M-CSF-activated human macrophages are highly efficient in ingesting small and large silica particles^[28] and others have recently reported that M2-polarized monocyte-derived macrophages are more prone to engulf gold nanoparticles.^[29] Hence, the cell model used here is highly proficient for phagocytosis and this could serve to explain the efficient uptake of small and large GO.

We observed that GO-S and GO-L both triggered the production of IL-17 and IFN- γ in macrophages, comparable to the effect of LPS on these cells, while TNF- α , an important proinflammatory cytokine, was not triggered by GO. In fact, LPS-induced TNF- α production in macrophages was reduced by GO. By contrast, Orecchioni et al.^[24] reported that GO triggered TNF- α , IL-1 β , and IL-10 secretion in peripheral blood mononuclear cells (PBMC) while IFN- γ was not affected. The same dose of GO (50 $\mu\text{g mL}^{-1}$) was used in both the latter study and the present study, and the discordant results serve to underscore

the importance of carefully considering the cell model, i.e., primary human monocyte-derived macrophages, with or without LPS priming, versus primary human PBMC, a pool of immune cells that includes both T cells, B cells, monocytes, dendritic cells (DC), and natural killer cells.^[24] Notably, while IL-17 and IFN- γ play key roles in host defense against pathogens, both cytokines have also been implicated in autoimmune diseases.^[48,49] One may speculate whether internalized GO sheets are sensed as intracellular parasites by macrophages, leading to IFN- γ secretion. IL-10, in turn, plays an important role in regulating IFN- γ secretion, thereby helping to curtail excessive immune responses that could lead to tissue damage and disease.^[50] Interestingly, our data showed that GO-S and GO-L potently suppressed bacterial LPS-induced secretion of IL-10 in macrophages. IL-10 is an essential immunomodulatory cytokine with multiple, pleiotropic effects and it is produced by almost all types of cells in the innate and adaptive immune system.^[32] IL-10 was originally described as an important negative regulator of immune responses to microbial antigens, preventing damage to the host. Loss of IL-10 leads to inflammatory diseases, most notably the development of inflammatory bowel disease.^[51] In addition to its “classical” anti-inflammatory properties, IL-10 also induces several essential mechanisms for effective antitumor immune surveillance.^[52–54] Thus, effects of GO on IL-10 production could have implications not only for host defense against pathogens, but could potentially also play a role in modulating immune surveillance against tumors. Further investigations on the regulation of IL-10 expression in immune cells exposed to GO are warranted and studies to evaluate a potential role of GO in regulating antitumor responses may also be of interest.

GO-S and GO-L also elicited effects on some chemokines (MCP-1/CCL2, MIP-1 β /CCL4), but not on others (MIP-1 α /CCL3, RANTES/CCL5, IP-10/CXCL10). GO-S and GO-L also abolished the production of RANTES/CCL5 and IP-10/CXCL10 in LPS-primed macrophages. Furthermore, we recently performed transcriptomics profiling of macrophages and could find no evidence of upregulation of chemokine-encoding genes in GO-exposed cells while single-walled CNTs triggered the expression of multiple different chemokines (Mukherjee et al., submitted for publication). It is worth noting that in a recent *in vivo* study, the expression of MCP-1 and MIP-1 β , but not MIP-1 α , was increased in the peritoneal exudate of mice following intraperitoneal injection of GO, with a concomitant increase in the level of infiltrating monocytes and a decrease in the number of macrophages.^[55] In another very recent study, intravenous injection of GO triggered the expression of MCP-1 in the lungs and kidneys of exposed mice at 24 h, but not at 10 d after injection.^[25] The current study using human monocyte-derived macrophages as a model is not directly comparable to the latter animal models, but the combined *in vitro* and *in vivo* results nevertheless suggest a similar response to GO with respect to chemokines.

Previous studies have shown that various carbon-based nanomaterials are capable of triggering caspase-1-dependent IL-1 β secretion in macrophages.^[21,34,35,56] The transcription of pro-IL-1 β is activated upon TLR stimulation, for example, by bacterial LPS, and LPS is often used to activate NF κ B-mediated transcription *in vitro* when assessing NLRP3 inflammasome

activation by exogenous substances.^[15] Palomäki et al.^[34] showed that multiwalled CNTs triggered IL-1 β secretion only in LPS-primed, but not in naïve primary human macrophages. Furthermore, these authors could show that NLRP3 was essential for CNT- and asbestos-induced IL-1 β secretion. In addition, we recently demonstrated that hollow carbon spheres triggered caspase-1-dependent IL-1 β secretion in primary human macrophages and found that cellular uptake was required for IL-1 β secretion.^[35] Similarly, classical caspase-1-dependent inflammasome activation by silica and aluminum salt crystals was shown to require phagocytosis of the crystals, subsequently leading to lysosomal damage and cathepsin B release.^[17] On the other hand, caspase-8 was shown to be involved in noncanonical fungal pathogen-triggered inflammasome activation occurring independently of internalization of the pathogen.^[57] Sun et al.^[38] reported that the NADPH oxidase is required for inflammasome activation in cells exposed to multiwalled CNTs, and provided evidence for a role of the NADPH oxidase for IL-1 β production *in vivo* using p47^{phox}-deficient mice. In the present study, we found that GO-S and GO-L both triggered IL-1 β secretion in LPS-primed primary human macrophages, but not in the absence of LPS priming, and we could demonstrate a role for caspase-1 as well as caspase-8. In addition, we could show that cellular uptake and NADPH oxidase-generated ROS was required for IL-1 β secretion. Cho et al.^[25] reported that IL-1 β production in THP-1 cells exposed to GO was influenced by phagocytosis in a size-dependent manner, but a specific role for the inflammasome was not demonstrated. Furthermore, we noted that GO-induced IL-1 β secretion was accompanied by lysosomal cathepsin B release and K⁺ efflux. As mentioned already, K⁺ efflux is a common feature of inflammasome activation by bacterial toxins and particulate matter (i.e., silica, aluminum, or calcium pyrophosphate crystals).^[36] Wang et al.^[21] also documented the lysosomal release of cathepsin B in THP-1 cells exposed to single-walled CNTs, graphene, and GO. Using knockdown cells, we could confirm a role for the inflammasome sensor, NLRP3, the adaptor protein, ASC, and the caspase-1 protease for GO-induced IL-1 β secretion, thus demonstrating that GO triggers canonical NLRP3 inflammasome activation.

Previous studies have identified the NLRP3 inflammasome as a crucial element in the adjuvant effect of aluminum adjuvants, the most commonly used adjuvants in human vaccines.^[19,58] Engineered nanomaterials are envisioned as elements of the next generation of vaccines, adjuvants, and immunomodulatory drugs.^[59] The current observation that GO triggers inflammasome activation in activated macrophages, in the absence of cell death, may suggest that GO could act not only as an antigen carrier, but also as an adjuvant, thereby boosting the immune response. Indeed, very recent studies have reported that surface-modified GO may be deployed as a highly effective antigen carrier for immunomodulation *in vivo*.^[60,61] Thus, while the present study was conducted *in vitro* using isolated human macrophages, and concentrations of GO (50 μ g mL⁻¹) that are likely in excess of the concentrations that may be achieved *in vivo*, the findings could nevertheless have implications for the potential use of GO in the clinical setting, and serve to shed light on the mechanisms underlying innate immune responses to GO. Further studies on other antigen-presenting cells including DCs^[62] may be of great interest.

Finally, it is interesting to note that the only difference in the present study between GO-S and GO-L was the fact that GO-S triggered a more rapid cathepsin B release from the lysosomal compartment when compared to GO-L. Similarly, Wang et al.^[21] found that GO can cause the release of cathepsin B in THP-1 cells, but the actual mechanism of lysosomal damage is not known. GO can be viewed essentially as a network of hydrophobic “islands” of unoxidized benzene rings surrounded by polar groups^[63] and small GO sheets are more hydrophilic than larger ones because of greater charge density.^[64] Interestingly, a very recent study revealed that high doses of GO (200 $\mu\text{g mL}^{-1}$ for 6 h) can produce pores in the plasma membrane of mammalian cells, and molecular dynamics simulations suggested that multiple nanosized graphene sheets can cooperate to extract phospholipids from membranes.^[65] Thus, although this remains to be tested, one may speculate that small GO within lysosomes could interact more strongly with lipids in the surrounding membrane via a similar cooperative mechanism, resulting in more rapid lysosomal damage and cathepsin B release when compared to larger sheets. However, as noted in the present study, both small and large GO sheets ultimately succeeded in triggering lysosomal cathepsin B release and subsequent caspase-dependent IL-1 β secretion in macrophages, and the overall responses to GO-S and GO-L were similar. Further to this point, it is of considerable interest to reflect on a recent study designed to assess why long and “stiff” (rigid) CNTs are more cytotoxic than short or flexible ones.^[66] In this study, the authors combined molecular dynamics simulations and in vitro cellular imaging to study CNT behavior in intracellular vesicles (i.e., lysosomes) and devised a classification diagram that distinguishes pathogenic from biocompatible nanomaterials based on a “nanomechanical buckling” criterion.^[66] The proposed classification is based on the geometric criteria for nanomaterials to induce lysosomal permeability through mechanical stress and could help to explain why long and rigid CNTs are more prone to cause cytotoxicity and lysosomal damage.^[67,68] It is tempting to speculate that similar mechanical properties could influence the behavior of GBMs; thus, single-layer GO may be less cytotoxic than few-layer GO based on differences in biological softness or buckling under lysosomal compressive forces. Indeed, in a recent study, multilayer GO was shown to be more cytotoxic in THP-1 cells than single-layer GO.^[25] However, detailed experimental and theoretical studies are required to address this. Furthermore, lipid extraction and/or oxidation by GO^[69–71] might also come into play, as shown in recent studies on bacterial membranes. At any rate, the present studies have provided evidence that single-layer GO is noncytotoxic for macrophages despite significant cellular uptake while TEM imaging showed that GO-S and GO-L were folded or “buckled” inside the cell.

4. Conclusions

In conclusion, in this study, we have shown that (i) both small and large GO sheets are readily engulfed by primary human macrophages; (ii) GO is not cytotoxic for primary human macrophages; (iii) GO does not appear to engage TLRs; (iv) GO per se does not trigger typical Th1 cytokines (i.e., TNF- α , IL-6,

or IL-1 β) or Th2 cytokines (i.e., IL-4, IL-5, and IL-13) in macrophages, but GO significantly suppresses several LPS-induced cytokines, including the anti-inflammatory cytokine, IL-10; (v) GO modulates the expression of IL-1 β and its antagonist, IL-1RA in macrophages; (vi) GO triggers caspase-1-dependent IL-1 β secretion, a hallmark of inflammasome activation, in LPS-primed macrophages; (vii) GO elicits canonical NLRP3–ASC–caspase-1-dependent IL-1 β secretion in LPS-primed cells; (viii) GO does not trigger size-dependent effects in macrophages. These results testify to the biocompatibility of endotoxin-free GO toward primary macrophages and call into the question the notion that GO is proinflammatory. The results may also have implications for biomedical applications of GO, e.g., in vaccination.

5. Experimental Section

GO Synthesis and Characterization: GO sheets of differing lateral dimensions were synthesized using a modified Hummers’ method as described^[27] under endotoxin-free conditions by using a laminar flow hood, endotoxin-free water, nonpyrogenic plastic containers, and depyrogenated glassware; in addition, gloves were used during the entire process to reduce skin contact.^[31] The structural properties of the small and large GO reconstituted in water, including lateral dimension and thickness, were studied by optical microscopy, TEM, and atomic force microscopy.^[26] In addition, zeta potential and size measurements by dynamic light scattering were performed both in deionized water (dH₂O) and in cell culture medium. Electrophoretic mobility (μ) was measured using Malvern Zetasizer Nano ZS (UK) after preparing the samples (GO-S and GO-L) at 50 $\mu\text{g mL}^{-1}$ in dH₂O and in RPMI-1640 medium supplemented with 10% fetal bovine serum (FBS) in disposable Zetasizer cuvettes (Malvern Instruments). The measurements were carried out at 25 °C, where the voltage was set at 10 V with automatic attenuation selection. Furthermore, automatic analysis was used for all measurements, where the μ was converted automatically by the equipment software to zeta potential (ζ) values. The hydrodynamic size of GO-S and GO-L was also measured at 50 $\mu\text{g mL}^{-1}$ in dH₂O versus serum-containing cell culture medium using default instrument settings and automatic analysis. All values are the average of six independent measurements.

Endotoxin Assessment: The endotoxin content in the GO samples was assessed using the TET as previously described.^[31] Briefly, primary human macrophages (see below) were exposed for 24 h to a noncytotoxic concentration (i.e., 50 $\mu\text{g mL}^{-1}$) of GO-S and GO-L as determined by using the Alamar Blue assay, in the presence and absence of the specific endotoxin inhibitor, polymyxin-B sulfate (10×10^{-6} M) (Sigma-Aldrich, Sweden). The cell medium of exposed cells was then collected and TNF- α was quantified using an ELISA (Invitrogen, Sweden) following the manufacturer’s instruction. Absorbance was measured at 450 nm using a plate reader (Infinite F200, Tecan, Switzerland). Results are expressed as pg/50 000 cells of released TNF- α , based on triplicate samples from three independent experiments using cells from different human donors. In addition, macrophages were exposed to different doses of LPS (100 pg mL⁻¹ to 100 ng mL⁻¹) to generate a standard curve.

Primary Human Monocyte-Derived Macrophages: PBMC were prepared from buffy coats obtained from healthy blood donors (Karolinska University Hospital, Stockholm, Sweden) by density gradient centrifugation using Lymphoprep (Axis-Shield, Oslo, Norway) as described before.^[72] Briefly, PBMCs were positively selected based on CD14 expression using CD14 MicroBeads (Miltenyi Biotec, Bergisch Gladbach, Germany). To obtain HMDM, CD14+ monocytes were cultured in RPMI-1640 medium (Gibco Invitrogen, Sweden) supplemented with 2×10^{-3} M L-glutamine, 100 IU mL⁻¹ penicillin, 100 mg mL⁻¹ streptomycin, 10% heat-inactivated FBS, and 50 ng mL⁻¹

recombinant M-CSF (Novakemi, Sweden) for 3 d. In some experiments, HMDM were primed with 100 ng mL^{-1} of bacterial LPS (Sigma-Aldrich) for 2 h prior to exposure.

Cytotoxicity Evaluation: Cell viability was assessed using the Alamar blue (AB) assay, based on the metabolic conversion of resazurin, a nonfluorescent indicator dye, to red-fluorescent resorufin in living cells (Thermo Fisher Scientific, Sweden). HMDM were first primed with $0.1 \text{ } \mu\text{g mL}^{-1}$ LPS for 2 h. Then, after washing the cells for four times with warm phosphate-buffered saline (PBS) ($37 \text{ }^\circ\text{C}$) the cells were exposed for 24 h in 96-well plates to GO-S or GO-L (up to $75 \text{ } \mu\text{g mL}^{-1}$) in RPMI-1640 cell culture medium supplemented with 10% FBS (without recombinant M-CSF), or to 5% dimethyl sulfoxide (DMSO) as a positive control for cell death. Then, the AB assay was performed according to the manufacturer's instruction. Briefly, exposure medium was removed, cells were rinsed with PBS and $100 \text{ } \mu\text{L}$ of AB medium (10% [v/v] solution of AlamarBlue reagent), prepared freshly in RPMI-1640 complete medium, were added to each well. After 2 h of incubation at $37 \text{ }^\circ\text{C}$, fluorescence was measured at the respective excitation and emission wavelength of 531 nm and 595 nm using a Tecan Infinite F200 plate reader (Tecan, Stockholm, Sweden). AB alone and cell culture medium alone were included as blanks. The experiment was performed with at least three biological replicates and six technical replicates for each concentration of GO. Results were expressed as percentage cell viability versus negative control, which was set as 100%. Potential interference of GO with the AB assay was evaluated in an acellular system by incubating $75 \text{ } \mu\text{g mL}^{-1}$ of each of the GO samples with the AB reagent for 2 h at $37 \text{ }^\circ\text{C}$; no interference was observed (data not shown).

Transmission Electron Microscopy: To study cell uptake, cells were exposed to GO-L or GO-S ($50 \text{ } \mu\text{g mL}^{-1}$) for 3 h in cell medium supplemented with 10% FBS and then washed with PBS, trypsinated, and centrifuged at 1000 rpm for 5 min and analyzed by TEM. Cells were fixed in 2% glutaraldehyde in 0.1 M sodium cacodylate buffer containing 0.1 M sucrose and $3 \times 10^{-3} \text{ M CaCl}_2$, pH 7.4. Samples were washed in buffer and postfixed in 2% osmium tetroxide in 0.07 M sodium cacodylate buffer containing $1.5 \times 10^{-3} \text{ M CaCl}_2$, pH 7.4, at $4 \text{ }^\circ\text{C}$ for 2 h, dehydrated in ethanol followed by acetone, and embedded in LX-112 (Ladd, Burlington, VT). Sections were contrasted with uranyl acetate followed by lead citrate and were examined in a Tecnai 12 Spirit Bio TWIN TEM (FEI, The Netherlands) at 100 kV. Digital images were taken using a Veleta camera (Olympus Soft Imaging Solutions, GmbH, Germany).

Cytokine-Chemokine Multiplex Profiling: To monitor cytokine-chemokine production, HMDM were preincubated or not with $0.1 \text{ } \mu\text{g mL}^{-1}$ LPS for 2 h. Then, the cells were exposed to $50 \text{ } \mu\text{g mL}^{-1}$ of GO-S or GO-L for 24 h, or to LPS ($0.1 \text{ } \mu\text{g mL}^{-1}$), and cell culture samples were collected, centrifuged at 12 000 rpm for 5 min to remove cell debris and stored at $-80 \text{ }^\circ\text{C}$ until analysis. Cytokine profiling was performed on cell culture supernatants using the 27-plex human suspension cyto/chemokine assay kit (Bio-Plex Human 27-Plex Cytokine from Bio-Rad Laboratories, Hercules, CA) as described.^[30] For analysis, samples were thawed and kept on ice. Samples were then measured using Bio-Plex 200 system (Luminex xMAP Technology) and Bio-Plex software (Bio-Rad Laboratories AB, Sundbyberg, Sweden). Cytokine standards were reconstituted in RPMI-1640 medium supplemented with 10% FBS. The experiments were performed using cells from three different blood donors, each tested in triplicate samples. The results are expressed as pg/30 000 cells of released cytokine, based on standard curves. The cytokine-chemokine expression data retrieved from the multiplex assay were analyzed using hierarchical clustering analysis, as previously described.^[73] Complete linkage and Euclidean distances were employed as metrics to draw association dendrograms between cytokines-chemokines and the different treatment conditions. Cluster analysis and heatmaps were obtained using R 3.2.2.^[74]

Interleukin-1 β Detection: HMDM were primed or not with LPS ($0.1 \text{ } \mu\text{g mL}^{-1}$) for 2 h and then exposed to GO ($50 \text{ } \mu\text{g mL}^{-1}$). The exposed cell media were collected and stored at $-80 \text{ }^\circ\text{C}$ for further analysis. IL-1 β release was determined by using a human IL-1 β ELISA kit (Invitrogen, Sweden) according to the manufacturer's instruction. Absorbance was measured at 450 nm using a Tecan Infinite F200 plate reader. Results

are expressed as pg/50 000 cells of released cytokine, based on at least three independent experiments using cells from different blood donors. To assess the role of caspases, cells were preincubated for 2 h with either Z-YVAD-FMK ($10 \times 10^{-6} \text{ M}$), Z-IETD-FMK ($20 \times 10^{-6} \text{ M}$), or zVAD-FMK ($20 \times 10^{-6} \text{ M}$) (R&D Systems, Minneapolis, MN). Then, the cells were exposed to GO-S or GO-L at $50 \text{ } \mu\text{g mL}^{-1}$ for 24 h in RPMI-1640 cell culture medium supplemented with 10% FBS. The exposed cell media were collected and IL-1 β quantification was done using ELISA as described above. To study the role of cell uptake, LPS-primed ($0.1 \text{ } \mu\text{g mL}^{-1}$, 2 h) HMDM were preincubated or not with the inhibitor of actin polymerization, cytochalasin-D ($10 \times 10^{-6} \text{ M}$) (Sigma-Aldrich) for 1 h. Then cells were exposed to GO-S or GO-L at $50 \text{ } \mu\text{g mL}^{-1}$ concentrations for 24 h after which the exposed cell media were collected. IL-1 β quantification was performed by using ELISA. To assess the role of NADPH oxidase activation in HMDM exposed to GO, LPS ($0.1 \text{ } \mu\text{g mL}^{-1}$) primed (2 h) HMDM were preincubated for 2 h with $10 \times 10^{-6} \text{ M}$ DPI (Sigma-Aldrich) and then exposed to GO-S or GO-L at $50 \text{ } \mu\text{g mL}^{-1}$ for 24 h. The exposed cell media were collected and IL-1 β was quantified using ELISA.

Lysosomal Cathepsin B Release: Lysosomal activation with release of cathepsin B was measured using the Magic Red-cathepsin B substrate from Immuno-Chemistry Technologies (Bloomington, MN). Briefly, HMDM were primed for 2 h with LPS ($0.1 \text{ } \mu\text{g mL}^{-1}$) and then exposed to GO-S or GO-L at $50 \text{ } \mu\text{g mL}^{-1}$ for the indicated time-points. Then, medium was removed and the cells were washed with warm PBS ($37 \text{ }^\circ\text{C}$). The cells were then stained with the Magic Red cathepsin B substrate in PBS for 1 h at $37 \text{ }^\circ\text{C}$ in 5% CO_2 . After the incubation the cells were washed with PBS and the fluorescence of Magic Red was measured at excitation/emission of 540/590 nm (bandwidth Ex./Em. $\pm 24/20 \text{ nm}$) using a plate reader (Tecan Infinite F200). The fluorescence intensity measured is directly proportional with the amount of cathepsin B released to the cytosol. The results are expressed as a percentage increase compared to the unexposed negative control cells, which was set at 0%.

Intracellular Potassium Measurements: Intracellular K^+ level was measured using the potassium (K^+) sensitive dye, PBFI-AM (Thermo Fisher Scientific). HMDM were primed for 2 h with LPS ($0.1 \text{ } \mu\text{g mL}^{-1}$) and then exposed to GO-S or GO-L at $50 \text{ } \mu\text{g mL}^{-1}$. Nigericin ($15 \times 10^{-6} \text{ M}$) (Sigma-Aldrich) was used as a positive control. Following exposure the cell medium was removed and the cells were washed with warm PBS ($37 \text{ }^\circ\text{C}$). The cells were then stained with PBFI-AM at $5 \times 10^{-6} \text{ M}$ in PBS for 1 h at $37 \text{ }^\circ\text{C}$ and 5% CO_2 . Following the incubation the cells were washed with PBS and the fluorescence of PBFI-AM was measured at excitation/emission of 360/465 nm (bandwidth $\pm 35 \text{ nm}$) using a spectrophotometer (Infinite F200, Tecan, Männedorf, Switzerland). The results are expressed as % decrease compared to unexposed negative control.

Reactive Oxygen Species Measurements: Intracellular ROS levels were measured using the H2DCFDA assay (Thermo Fisher Scientific). Briefly, HMDM were seeded in black 96-well plates with transparent bottom at a density of 5×10^4 cells per well. Cells were primed with LPS ($0.1 \text{ } \mu\text{g mL}^{-1}$ for 2h) and then preloaded with $10 \times 10^{-6} \text{ M}$ H2DCFDA in PBS for 1 h min at $37 \text{ }^\circ\text{C}$ and 5% CO_2 . Then, cells were washed thrice with PBS and exposed to $50 \text{ } \mu\text{g mL}^{-1}$ of GO-S or GO-L. Fluorescence was recorded at $37 \text{ }^\circ\text{C}$ (excitation 485 nm, emission 535 nm) using a plate reader (Tecan Infinite F200). The results were plotted as % ROS generation in HMDM incubated in medium alone (set at 0%).

TLR Reporter Cell Lines: HEK 293 cells cotransfected with human TLR2 (HEK-Blue hTLR2) or TLR4 (HEK-Blue hTLR4 cells) and an NF- κB /AP-1-SEAP reporter gene were obtained from InvivoGen (Toulouse, France). Once TLR signaling is initiated, NF- κB and AP-1 is activated, which initiates the secretion of SEAP which can be detected in the cell supernatants to quantify NF- κB activation. The HEK-Blue Null1 cells were included as a negative control. HEK-Blue Null1, hTLR2, and hTLR4 cells were cultured in Dulbecco's modified Eagle's medium (DMSO) growth medium containing 4.5 g L^{-1} glucose and supplemented with 10% FBS, 50 U mL^{-1} penicillin, 50 mg mL^{-1} streptomycin, 100 mg mL^{-1} Normocin, $2 \times 10^{-3} \text{ M L}$ -glutamine and 1X HEK-Blue selection antibiotics mixture, according to the manufacturers' instruction. For Null1 cells, Zeocin was

used instead of the selection antibiotics mixture. Cells (2×10^5 cells mL⁻¹) were exposed for 12 h to 50 µg mL⁻¹ of GO-S or GO-L, or LPS (0.1 µg mL⁻¹) as a positive control, in HEK-Blue detection medium (InvivoGen). SEAP activity was measured at 630 nm using an Infinite F200 Tecan plate reader.

THP-1 Knockdown Cell Lines: Four different THP-1 monocytic cell lines (Null-1, defASC, defNLRP3, and defCaspase-1) were obtained from InvivoGen (France). The THP-1 null and knockdown cells^[75] were cultured according to the manufacturers' instructions. After sub-culturing the cells thrice in RPMI-1640 cell medium supplemented with 10% FBS, cells were seeded in 96-well plates at a density of 10^5 cells per well. Hygromycin B (Sigma-Aldrich) ($100 \mu\text{g mL}^{-1}$) was added for the knockdown cells. After 24 h, cells were primed or not with $0.1 \mu\text{g mL}^{-1}$ LPS for 2 h. Then, the cells were washed with PBS and exposed for 24 h to $50 \mu\text{g mL}^{-1}$ of GO-S or GO-L in 10% FBS-supplemented growth medium. Following incubation, cell culture media were collected and IL-1β content was measured using a specific ELISA.

Statistics: All experiments were conducted at least in triplicate (three independent experiments or biological replicates), where each biological replicate has 3–6 technical replicates. Statistical significance was tested with unpaired two-tailed Student *t*-test or one-way ANOVA with Tukey correction using GraphPad Prism version 5.02 for Windows (GraphPad Software, San Diego, CA). Data are reported as mean values ± S.D. or S.E.M.

Supporting Information

Supporting Information is available from the Wiley Online Library or from the author.

Acknowledgements

This work was supported by the European Commission, GRAPHENE Flagship Project (grant agreement nos. 604391 and 696656) and the Swedish Research Council (senior investigator award for inflammation research to B.F.). The authors thank Dr. Kunal Bhattacharya, Karolinska Institutet, for advice on cytokine data analysis, and Dr. Kjell Hultenby, Electron Microscopy Core Facility, Karolinska Institutet, for excellent assistance with TEM imaging.

Conflict of Interest

The authors declare no conflict of interest.

Keywords

cytokine profiling, graphene oxide, inflammasome, macrophages, polarization

Received: July 7, 2017

Revised: October 16, 2017

Published online: December 21, 2017

[1] A. C. Ferrari, F. Bonaccorso, V. Fal'ko, K. S. Novoselov, S. Roche, P. Bøggild, S. Borini, F. H. Koppens, V. Palermo, N. Pugno, J. A. Garrido, R. Sordan, A. Bianco, L. Ballerini, M. Prato, E. Lidorikis, J. Kivioja, C. Marinelli, T. Ryhänen, A. Morpurgo, J. N. Coleman, V. Nicolosi, L. Colombo, A. Fert, M. Garcia-Hernandez, A. Bachtold, G. F. Schneider, F. Guinea,

- C. Dekker, M. Barbone, Z. Sun, C. Galiotis, A. N. Grigorenko, G. Konstantatos, A. Kis, M. Katsnelson, L. Vandersypen, A. Loiseau, V. Morandi, D. Neumaier, E. Treossi, V. Pellegrini, M. Polini, A. Tredicucci, G. M. Williams, B. H. Hong, J. H. Ahn, J. M. Kim, H. Zirath, B. J. van Wees, H. van der Zant, L. Occhipinti, A. Di Matteo, I. A. Kinloch, T. Seyller, E. Quesnel, X. Feng, K. Teo, N. Rupesinghe, P. Hakonen, S. R. Neil, Q. Tannock, T. Löfwander, J. Kinaret, *Nanoscale* **2015**, *7*, 4598.
- [2] D. Bitounis, H. Ali-Boucetta, B. H. Hong, D. H. Min, K. Kostarelos, *Adv. Mater.* **2013**, *25*, 2258.
- [3] K. Bhattacharya, S. P. Mukherjee, A. Gallud, S. C. Burkert, S. Bistarelli, S. Bellucci, M. Bottini, A. Star, B. Fadeel, *Nanomedicine* **2016**, *12*, 333.
- [4] S. P. Mukherjee, B. Massimo, B. Fadeel, *Front. Immunol.* **2017**, *8*, 673.
- [5] K. Bhattacharya, F. T. Andón, R. El-Sayed, B. Fadeel, *Adv. Drug Delivery Rev.* **2013**, *65*, 2087.
- [6] F. Ginhoux, J. L. Schultze, P. J. Murray, J. Ochando, S. K. Biswas, *Nat. Immunol.* **2016**, *17*, 34.
- [7] C. D. Mills, K. Kincaid, J. M. Alt, M. J. Heilman, A. M. Hill, *J. Immunol.* **2000**, *164*, 6166.
- [8] P. J. Murray, J. E. Allen, S. K. Biswas, E. A. Fisher, D. W. Gilroy, S. Goerdts, S. Gordon, J. A. Hamilton, L. B. Ivashkiv, T. Lawrence, M. Locati, A. Mantovani, F. O. Martinez, J. L. Mege, D. M. Mosser, G. Natoli, J. P. Saeij, J. L. Schultze, K. A. Shirey, A. Sica, J. Suttles, I. Udalova, J. A. van Genderachter, S. N. Vogel, T. A. Wynn, *Immunity* **2014**, *41*, 14.
- [9] A. Sica, A. Mantovani, *J. Clin. Invest.* **2012**, *122*, 787.
- [10] X. Miao, X. Leng, Q. Zhang, *Int. J. Mol. Sci.* **2017**, *18*, pii: E336.
- [11] S. W. Jones, R. A. Roberts, G. R. Robbins, J. L. Perry, M. P. Kai, K. Chen, T. Bo, M. E. Napier, J. P. Ting, J. M. Desimone, J. E. Bear, *J. Clin. Invest.* **2013**, *123*, 3061.
- [12] E. Witasz, N. Kupferschmidt, L. Bengtsson, K. Hultenby, C. Smedman, S. Paulie, A. E. Garcia-Bennett, B. Fadeel, *Toxicol. Appl. Pharmacol.* **2009**, *239*, 306.
- [13] A. Kunzmann, B. Andersson, C. Vogt, N. Feliu, F. Ye, S. Gabrielsson, M. S. Toprak, T. Buerki-Thurnherr, S. Laurent, M. Vahter, H. Krug, M. Muhammed, A. Scheynius, B. Fadeel, *Toxicol. Appl. Pharmacol.* **2011**, *253*, 81.
- [14] F. Martinon, K. Burns, J. Tschopp, *Mol. Cell.* **2002**, *10*, 417.
- [15] P. Broz, V. M. Dixit, *Nat. Rev. Immunol.* **2016**, *16*, 407.
- [16] C. Dostert, V. Pétrilli, R. Van Bruggen, C. Steele, B. T. Mossman, J. Tschopp, *Science* **2008**, *320*, 674.
- [17] V. Hornung, F. Bauernfeind, A. Halle, E. O. Samstad, H. Kono, K. L. Rock, K. A. Fitzgerald, E. Latz, *Nat. Immunol.* **2008**, *9*, 847.
- [18] S. L. Cassel, S. C. Eisenbarth, S. S. Iyer, J. J. Sadler, O. R. Colegio, L. A. Tephly, A. B. Carter, P. B. Rothman, R. A. Flavell, F. S. Sutterwala, *Proc. Natl. Acad. Sci. USA* **2008**, *105*, 9035.
- [19] S. C. Eisenbarth, O. R. Colegio, W. O'Connor, F. S. Sutterwala, R. A. Flavell, *Nature* **2008**, *453*, 1122.
- [20] C. Farrera, B. Fadeel, *Eur. J. Pharm. Biopharm.* **2015**, *95*, 3.
- [21] X. Wang, M. C. Duch, N. Mansukhani, Z. Ji, Y. P. Liao, M. Wang, H. Zhang, B. Sun, C. H. Chang, R. Li, S. Lin, H. Meng, T. Xia, M. C. Hersam, A. E. Nel, *ACS Nano* **2015**, *9*, 3032.
- [22] A. Sasidharan, L. S. Panchakarla, A. R. Sadanandan, A. Ashokan, P. Chandran, C. M. Girish, D. Menon, S. V. Nair, C. N. Rao, M. Koyakutty, *Small* **2012**, *8*, 1251.
- [23] J. Ma, R. Liu, X. Wang, Q. Liu, Y. Chen, R. P. Valle, Y. Y. Zuo, T. Xia, S. Liu, *ACS Nano* **2015**, *9*, 10498.
- [24] M. Orecchioni, D. A. Jasim, M. Pescatori, R. Manetti, C. Fozza, F. Sgarrella, D. Bedognetti, A. Bianco, K. Kostarelos, L. G. Delogu, *Adv. Healthcare Mater.* **2016**, *5*, 276.
- [25] Y. C. Cho, P. J. Pak, Y. H. Joo, H. S. Lee, N. Chung, *Sci. Rep.* **2016**, *6*, 38884.

- [26] S. P. Mukherjee, B. Lazzaretto, K. Hultenby, L. Newman, A. F. Rodrigues, N. Lozano, K. Kostarelos, P. Malmberg, B. Fadeel, *Chem.* **2017**, in press.
- [27] H. Ali-Boucetta, D. Bitounis, R. Raveendran-Nair, A. Servant, J. Van den Bossche, K. Kostarelos, *Adv. Healthcare Mater.* **2013**, *2*, 433.
- [28] A. Gallud, O. Bondarenko, N. Feliu, N. Kupferschmidt, R. Atluri, A. Garcia-Bennett, B. Fadeel, *Biomaterials* **2017**, *121*, 28.
- [29] S. A. MacParland, K. M. Tsoi, B. Ouyang, X. Z. Ma, J. Manuel, A. Fawaz, M. A. Ostrowski, B. A. Alman, A. Zilman, W. C. Chan, I. D. McGilvray, *ACS Nano* **2017**, *11*, 2428.
- [30] Y. Li, D. Boraschi, *Nanomedicine (London, U. K.)* **2016**, *11*, 269.
- [31] S. P. Mukherjee, N. Lozano, M. Kucki, A. E. Del Rio-Castillo, L. Newman, E. Vázquez, K. Kostarelos, P. Wick, B. Fadeel, *PLoS One* **2016**, *11*, e0166816.
- [32] M. Saraiva, A. O'Garra, *Nat. Rev. Immunol.* **2010**, *10*, 170.
- [33] C. Antonopoulos, H. M. Russo, C. El Sanadi, B. N. Martin, X. Li, W. J. Kaiser, E. S. Mocarski, G. R. Dubyak, *J. Biol. Chem.* **2015**, *290*, 20167.
- [34] J. Palomäki, E. Välimäki, J. Sund, M. Vippola, P. A. Clausen, K. A. Jensen, K. Savolainen, S. Matikainen, H. Alenius, *ACS Nano* **2011**, *5*, 6861.
- [35] F. T. Andón, S. P. Mukherjee, I. Gessner, L. Wortmann, L. Xiao, K. Hultenby, A. A. Shvedova, S. Mathur, B. Fadeel, *Carbon* **2017**, *113*, 243.
- [36] R. Muñoz-Planillo, P. Kuffa, G. Martínez-Colón, B. L. Smith, T. M. Rajendiran, G. Núñez, *Immunity* **2013**, *38*, 1142.
- [37] G. Qu, S. Liu, S. Zhang, L. Wang, X. Wang, B. Sun, N. Yin, X. Gao, T. Xia, J. J. Chen, G. B. Jiang, *ACS Nano* **2013**, *7*, 5732.
- [38] B. Sun, X. Wang, Z. Ji, M. Wang, Y. P. Liao, C. H. Chang, R. Li, H. Zhang, A. E. Nel, T. Xia, *Small* **2015**, *11*, 2087.
- [39] M. Lucarelli, A. M. Gatti, G. Savarino, P. Quattroni, L. Martinelli, E. Monari, D. Boraschi, *Eur. Cytokine Network* **2004**, *15*, 339.
- [40] V. Kodali, M. H. Littke, S. C. Tilton, J. G. Teeguarden, L. Shi, C. W. Frevert, W. Wang, J. G. Pounds, B. D. Thrall, *ACS Nano* **2013**, *7*, 6997.
- [41] A. K. Fuchs, T. Syrovets, K. A. Haas, C. Loos, A. Musyanovych, V. Mailänder, K. Landfester, T. Simmet, *Biomaterials* **2016**, *85*, 78.
- [42] Y. Li, P. Italiani, E. Casals, D. Valkenborg, I. Mertens, G. Baggerman, I. Nelissen, V. F. Puentes, D. Boraschi, *ACS Appl. Mater. Interfaces* **2016**, *8*, 28437.
- [43] S. Mittal, V. Kumar, N. Dhiman, L. K. Chauhan, R. Pasricha, A. K. Pandey, *Sci. Rep.* **2016**, *6*, 39548.
- [44] O. N. Ruiz, K. A. Fernando, B. Wang, N. A. Brown, P. G. Luo, N. D. McNamara, M. Vangsness, Y. P. Sun, C. E. Bunker, *ACS Nano* **2011**, *5*, 8100.
- [45] Kenry, P. K. Chaudhuri, K. P. Loh, C. T. Lim, *ACS Nano* **2016**, *10*, 3424.
- [46] J. Russier, E. Treossi, A. Scarsi, F. Perrozzi, H. Dumortier, L. Ottaviano, M. Meneghetti, V. Palermo, A. Bianco, *Nanoscale* **2013**, *5*, 11234.
- [47] A. Aderem, D. M. Underhill, *Annu. Rev. Immunol.* **1999**, *17*, 593.
- [48] F. McNab, K. Mayer-Barber, A. Sher, A. Wack, A. O'Garra, *Nat. Rev. Immunol.* **2015**, *15*, 87.
- [49] M. Veldhoen, *Nat. Immunol.* **2017**, *18*, 612.
- [50] A. Cope, G. Le Friec, J. Cardone, C. Kemper, *Trends Immunol.* **2011**, *32*, 278.
- [51] R. Kühn, J. Löhler, D. Rennick, K. Rajewsky, W. Müller, *Cell* **1993**, *75*, 263.
- [52] J. B. Mumm, J. Emmerich, X. Zhang, I. Chan, L. Wu, S. Mauze, S. Blaisdell, B. Basham, J. Dai, J. Grein, C. Sheppard, K. Hong, C. Cutler, S. Turner, D. LaFace, M. Kleinschek, M. Judo, G. Ayanoglu, J. Langowski, D. Gu, B. Paporello, E. Murphy, V. Sriram, S. Naravula, B. Desai, S. Medicherla, W. Seghezzi, T. McClanahan, S. Cannon-Carlson, A. M. Beebe, M. Oft, *Cancer Cell.* **2011**, *20*, 781.
- [53] R. M. Berman, T. Suzuki, H. Tahara, P. D. Robbins, S. K. Narula, M. T. Lotze, *J. Immunol.* **1996**, *157*, 231.
- [54] L. M. Zheng, D. M. Ojcius, F. Garaud, C. Roth, E. Maxwell, Z. Li, H. Rong, J. Chen, X. Y. Wang, J. J. Catino, I. King, *J. Exp. Med.* **1996**, *184*, 579.
- [55] S. A. Sydlík, S. Jhunjunwala, M. J. Webber, D. G. Anderson, R. Langer, *ACS Nano* **2015**, *9*, 3866.
- [56] F. Jessop, A. Holian, *Nanotoxicology* **2015**, *9*, 365.
- [57] S. I. Gringhuis, T. M. Kaptein, B. A. Wevers, B. Theelen, M. van der Vlist, T. Boekhout, T. B. Geijtenbeek, *Nat. Immunol.* **2012**, *13*, 246.
- [58] H. Li, S. B. Willingham, J. P. Ting, F. Re, *J. Immunol.* **2008**, *181*, 17.
- [59] D. M. Smith, J. K. Simon, J. R. Baker, *Nat. Rev. Immunol.* **2013**, *13*, 592.
- [60] L. Xu, J. Xiang, Y. Liu, J. Xu, Y. Luo, L. Feng, Z. Liu, R. Peng, *Nanoscale* **2016**, *8*, 3785.
- [61] C. Meng, X. Zhi, C. Li, C. Li, Z. Chen, X. Qiu, C. Ding, L. Ma, H. Lu, D. Chen, G. Liu, D. Cui, *ACS Nano* **2016**, *10*, 2203.
- [62] H. Li, K. Fierens, Z. Zhang, N. Vanparijs, M. J. Schuijs, K. Van Steendam, N. Feiner Gracia, R. De Rycke, T. De Beer, A. De Beuckelaer, S. De Koker, D. Deforce, L. Albertazzi, J. Grooten, B. N. Lambrecht, B. G. De Geest, *ACS Appl. Mater. Interfaces* **2016**, *8*, 1147.
- [63] S. Wang, Y. Zhang, N. Abidi, L. Cabrales, *Langmuir* **2009**, *25*, 11078.
- [64] J. Kim, L. J. Cote, F. Kim, W. Yuan, K. R. Shull, J. Huang, *J. Am. Chem. Soc.* **2010**, *132*, 8180.
- [65] G. Duan, Y. Zhang, B. Luan, J. K. Weber, R. W. Zhou, Z. Yang, L. Zhao, J. Xu, J. Luo, R. Zhou, *Sci. Rep.* **2017**, *7*, 42767.
- [66] W. Zhu, A. von dem Bussche, X. Yi, Y. Qiu, Z. Wang, P. Weston, R. H. Hurt, A. B. Kane, H. Gao, *Proc. Natl. Acad. Sci. USA* **2016**, *113*, 12374.
- [67] J. Palomäki, J. Sund, M. Vippola, P. Kinaret, D. Greco, K. Savolainen, A. Puustinen, H. Alenius, *Nanotoxicology* **2015**, *9*, 719.
- [68] H. Nagai, Y. Okazaki, S. H. Chew, N. Misawa, Y. Yamashita, S. Akatsuka, T. Ishihara, K. Yamashita, Y. Yoshikawa, H. Yasui, L. Jiang, H. Ohara, T. Takahashi, G. Ichihara, K. Kostarelos, Y. Miyata, H. Shinohara, S. Toyokuni, *Proc. Natl. Acad. Sci. USA* **2011**, *108*, E1330.
- [69] Y. Tu, M. Lv, P. Xiu, T. Huynh, M. Zhang, M. Castelli, Z. Liu, Q. Huang, C. Fan, H. Fang, R. Zhou, *Nat. Nanotechnol.* **2013**, *8*, 594.
- [70] V. T. Pham, V. K. Truong, M. D. Quinn, S. M. Notley, Y. Guo, V. A. Baulin, M. Al Kobaisi, R. J. Crawford, E. P. Ivanova, *ACS Nano* **2015**, *9*, 8458.
- [71] R. Li, N. D. Mansukhani, L. M. Guiney, Z. Ji, Y. Zhao, C. H. Chang, C. T. French, J. F. Miller, M. C. Hersam, A. E. Nel, T. Xia, *ACS Nano* **2016**, *10*, 10966.
- [72] N. Feliu, M. V. Walter, M. I. Montanez, A. Kunzmann, A. Hult, A. Nyström, M. Malkoch, B. Fadeel, *Biomaterials* **2012**, *33*, 1970.
- [73] K. Bhattacharya, G. Kilic, P. M. Costa, B. Fadeel, *Nanotoxicology* **2017**, *11*, 809.
- [74] R. Ihaka, R. Gentleman, *J. Comput. Graph. Stat.* **1995**, *5*, 299.
- [75] A. Naji, B. A. Muzembo, K. Yagyu, N. Baba, F. Deschaseaux, L. Sensebé, N. Suganuma, *Sci. Rep.* **2016**, *6*, 26162.